# Surface Engineering in Alloyed CdSe/CdSe$_x$CdS$_{1-x}$/CdS Core-Shell Colloidal Quantum Dots for Enhanced Optoelectronic Applications

**Sidney A. Lourenço, Anielle Christine A. Silva, Victor M. Zelaya, Carlos E. Cava, Gabriel D. A. Rocha, Marco A. T. da Silva, José L. Duarte, Flavio Franchello, Felipe de Almeida La Porta and Noelio O. Dantas**

**Abstract** The optical properties of nanocrystal (NC) colloidal quantum dots (QDs) largely depend on their size and shape. These properties can be easily tuned by temperature and the concentration of ligands during their synthesis to generate QD particles with different optical features. However, the enormous complexity of these QD systems limits the understanding of the critical impact of passivating ligands and surface defects on their optical properties. In the present study, we systematically investigated the effect of different strategies on the optical properties of alloyed CdSe/CdSe$_x$CdS$_{1-x}$/CdS core shell (CS) QDs capped with several ligands, including trioctylphosphine (TOP) and hexadecylamine (HDA). The CdSe covered with TOP ligands were produced using the hot injection method, whereas CdSe covered with HDA ligands were produced by the exchange reaction method from as-synthesized samples. The CdSe/CdSe$_x$CdS$_{1-x}$/CdS QDs samples were prepared from a simple chemical route that involved an increasing concentration of thioglycerol to grow the CdS shell on the top of the as-precipitated CdSe core with different ligands in a controlled manner. Two emission peaks (at approximately 595 and 635 nm) were observed for three different surface coverages beyond the exciton recombination. These emissions were mainly attributed to the surface localized state

S. A. Lourenço · C. E. Cava · G. D. A. Rocha · M. A. T. da Silva
Laboratório de Dispositivos Fotônicos e Materiais Nanoestruturados, Universidade
Tecnológica Federal do Paraná – UTFPR, 86036-370 Londrina, PR, Brazil

A. C. A. Silva · N. O. Dantas
Laboratório de Novos Materiais Isolantes e Semicondutores (LNMIS),
Instituto de Física, Universidade Federal de Uberlândia, CP 593, 38400-902
Uberlândia, MG, Brazil

V. M. Zelaya · J. L. Duarte · F. Franchello
Departamento de Física, Universidade Estadual de Londrina, 86051-970 Londrina, PR, Brazil

F. A. La Porta (✉)
Laboratório de Nanotecnologia e Química Computacional, Universidade Tecnológica
Federal do Paraná – UTFPR, 86036-370 Londrina, PR, Brazil
e-mail: felipelaporta@utfpr.edu.br

in all samples and the charge carrier transfer between the exciton and surface states. Our findings revealed an increase in the photoluminescence (PL) intensity with increasing temperature for the alloyed CdSe/CdSe$_x$CdS$_{1-x}$/CdS CS QDs. The findings also revealed a continuous red-shift in the optical absorption peak, as a function of ligand concentration. This suggests a strong electronic coupling between the surface localized states and delocalized excitonic alloyed CdSe/CdSe$_x$CdS$_{1-x}$/CdS CS QDs. However, such colloidal nanocrystals (NCs) need to be further investigated to gain an in-depth understanding of their nanoscale behavior as well as explore their huge potential for several emerging technological applications.

**Keywords** Colloidal quantum dots · Surface states · Passivating ligands · Charge carrier transfer

# 1   Introduction

In recent decades, nanocrystalline colloidal quantum dots (QDs) have emerged as a promising option for several optoelectronic technologies, owing to the continuous tunability of their electronic and optical properties, which, in turn, results from the ease of alteration of their size, shape, and surface [1–6]. Moreover, novel physical properties of QDs have demonstrated potential applications in different technologic areas, such as light-emitting devices (LEDs) [7–10], low-threshold lasers [11], optical amplifiers [12], photovoltaic devices [13–16] field-effect transistors (FETs) [17], biological labels [18–20], antibacterial control [21], and cancer therapy [22].

The extremely small size of QDs, in the range of nanoscale, confers the property of a high surface-to-volume ratio to them, such that majority of the atoms are located on the surface [23]. The atoms at the surface of QDs can generate diverse surface defect sites (e.g., dangling bonds) that act as trap sites for charged carriers. For example, the trapping of charge carriers at the surface defect sites results in an exciton delocalization that may theoretically cause non-radiative recombination pathways with low photoluminescence quantum yields (PLQYs) [5, 24, 25]. These adverse effects may decrease the performance of several optoelectronic devices based on QDs systems [5, 24, 25]. Thus, intense efforts are being made to understand the role of charge carrier trapping at surface defects in physical processes such as carrier relaxation and recombination dynamics, which can provide great opportunities in the field of nanotechnology. However, knowledge related to surface trapping is still limited with several questions remaining unanswered [26–28].

A frequent method used to reduce the number of defect states and dangling bonds present on the nanocrystal (NC) surface, and thus the exciton delocalization, is the direct passivation of the QD surface with organic ligands, such as hexadecylamine (HDA), thioglycolic acid (TGA), mercaptopropionic acid (MPA), and trioctylphosphine (TOP). It has been demonstrated that the passivation of QD systems with organic capping agents strongly influences the electron and hole transport from QDs. Thus, passivation acts as a critical factor for the delivery of

photoexcited carriers in photovoltaic devices [5, 29–31], and in biomedical and clinical imaging applications [20, 32, 33].

Another method used to reduce surface trap states is the synthesis of core/shell structures. Here, two materials with different energy band gaps are used, thus creating a potential barrier at the semiconductor interface. This can increase the confinement potential of the charge carriers in the core region. That is, if the core QD gets encapsulated by another system of interest as a shell with a wide band gap, this generates two possibilities of alignment to confine either both (type-I) or a single (quasi-type-II) charge carrier to the core and minimize their surface overlap [34, 35]. However, the abrupt boundary between the core and shell materials can also induce strain owing to lattice mismatch and hence introduce new trap states at the core/shell interface [36]. Thus, recently it was proposed that a thick-graded shell could be considered as an efficient strategy to cover the semiconductor QD core and provide better enhancement of fluorescence with a significant impact on light-emitting devices (e.g., PLQY greater than 90% has been observed for such systems) [35, 36]. This particular structure has been shown to reduce Auger recombination, a non-radiative process, in semiconductor QDs, particularly the graded alloyed CdSe/CdSe$_x$CdS$_{1-x}$/CdS system; delocalize the electron into the *thick* CdS shell; reduce its overlap with the core-localized hole; [37] and improve the multi-exciton performance of the complex QD [30, 38, 39]. Hence, different strategies based on *inorganic or organic* surface cover have been employed to improve the PLQY, as well as, facilitate the charge energy transfer process in QD-based optical devices [27, 40, 41].

Thus, in the present work, we used steady-state photoluminescence (PL) as a function of temperature and time-resolved PL to study the electronic coupling between surfaces and excitonic states in three sets of CdSe QDs covered with different ligands. The set-1 (as-synthesized QDs) consisted of five samples of CdSe QDs with the size ranging from 2.16 to 2.46 nm and covered by TOP molecules. The set-2 consisted of five samples of CdSe QDs (the same of set-1) but functionalized, after exchange reaction process, with HDA molecules. The set-3, was proposed by Silva et al. [42], and resulted from a novel methodology to grow core-shell quantum dots (CS-QDs), using an aqueous-based wet chemistry protocol, in which the thickness of the CdS shell could be controlled by tuning the thioglycerol concentration. This system, with a *thin*-graded CdSe$_x$S$_{1-x}$/CdS shell, which allowed surface states from 1-thioglycerol residual ligand to strongly couple with confined states, led to a strong quenching of excitonic recombination.

## 2   Samples and Experimental Section

The synthesis of CS-QDs was carried out by using an aqueous-based wet chemistry protocol. The proposed chemical route uses increasing concentration of 1-thioglycerol, a bifunctional linker molecule, (**HS**-CH$_2$CH$_2$**COOH**) to grow the CdS shell on top of the as-precipitated CdSe core in a controllable way. It was found

that lower concentration of 1-thioglycerol (3 mmol) added into the reaction medium limits the growth of the CdSe core, and to higher concentration (5–11 mmol) of 1-thioglycerol (TG) promotes the growth of CdS shell on top of the CdSe core with an increase from 0.50 to 1.25 nm in shell thickness. More details about synthesis methodology can be obtained in the following Ref. [42]. Briefly, CdSe QDs and CdSe/CdSe$_x$S$_{1-x}$/CdS CS-QDs were grown in aqueous solutions at room temperature using the following steps. Selenium powder (mmol, 99.999%), and a strong reduction agent, sodium Borohydride NaBH$_4$ (mmol, 98%), were dispersed in ultrapure water (20 mL) in a three-neck flask under argon flow. After that, 2 mmol of Cd(ClO$_4$)$_2$. 6H$_2$O and x mmol of 1-thioglycerol were mixed in ultrapure water, and the pH was adjusted to 11 by adding 0.1 M NaOH. Then, cadmium- and selenium-containing solutions were mixed under magnetic stirring in a three-neck flask under argon flow at room temperature for 30 min. CdSe QDs and CdSe/CdSe$_x$S$_{1-x}$/CdS CS-QDs were precipitated with ethanol and centrifuged four times at 6000 rpm for 10 min. In this procedure, a thin intermediary alloy of CdSe$_x$S$_{1-x}$ is formed on CdSe QDs. The confirmation of the CdSe$_x$S$_{1-x}$ alloying, while using 1-thioglycerol, was supported by the change of the bandwidth value related to the LO branch with respect to bulk CdSe ($\Delta\omega = 118$ cm$^{-1}$) [42]. The resulting nanopowders were dried in vacuum (mechanical pump) at room temperature and further dispersed in ultrapure water. With increasing TG concentration, five samples were obtained, which were analyzed in this paper. They were labeled as: CdSe:1TG, this sample has CdSe core with average size of 1.9 nm; CdSe:5TG, CdSe/CdS core-shell with core size of 1.7 nm and shell size of 0.514 nm; CdSe:7TG, CdSe/CdS core-shell with core size of 1.7 nm and shell size of 0.665 nm; CdSe:9TG, CdSe/CdS core-shell with core size of 1.7 nm and shell size of 0.869 nm and CdSe:11TG, CdSe/CdS core-shell with core size of 1.7 nm and shell size of 0.975 nm. Sizes of the core and shell were obtained from the analysis of optical absorption, X-ray diffraction and Raman techniques [42].

After synthesis, evaporation processes were initialized to obtain CS-QDs in a powder form. Photoluminescence (PL) was measured with a 405 nm ($\sim$3.06 eV) continuous wave laser focused at $\sim$200 μm and with low excitation power, 1.34 mW. These powders were put into a circular cavity of copper-cold finger closed by a quartz window. Luminescence spectra were collected from 15 to 300 K using a USB4000 Ocean Optics spectrometer equipped with a Toshiba TCD1304AP 3648-element linear CCD-array detector and a GG 435 nm long-wave-pass filter. Sample temperatures were controlled by a closed-cycle He cryostat (Janis, model CCS—150) equipped with a Lake Shore temperature controller (Model 805). Photoluminescence decay time measurements were performed by a Picoquant system (Fluotime 200), with a time-correlated single photon counting (TCSPC) technique, equipped with a MCP detector. For this measurement, samples were diluted in 23 mg/mL of deionized water. A picosecond pulsed diode laser (at 440 nm), 2.5 MHz repetition rate, 55 ps pulse, was used as excitation source.

For comparation purpose, it was synthesized five as-synthesized CdSe, covered with TOP molecules, with different size and other five CdSe QDs surface-stabilized

with HDA, both diluted in toluene. The CdSe QDs were synthesized via the hot injection method [43]. It begins with the preparation of two solutions: a solution of TOP-Se and other of Cd. In the preparation of the first solution, 30 mg of Se and 5.0 ml of octadecene were added in a 10 ml flask on inert atmosphere (Ar gas). Then, it is adding 0.40 mL of TOP via a syringe. In this stage, the solution temperature was mantled at 100 °C. For the second solution, it was added 13 mg of CdO, 0.60 mL oleic acid (OA) and 10 ml of octadecene in a three-necked flask. This process should also be in an inert atmosphere to prevent the O$_2$ released to not oxidize the TOP when the first solution is injected. When the temperature of the second solution reaches 225 °C, it is injected TOP-Se within the Cd precursor solution to induce nucleation and nanoparticle growth. In this route synthesis, the TOP cap is grown on CdSe surface, which protect the CdSe QD. All reagents used in the synthesis procedure were purchased from Sigma-Aldrich (Brazil) and used without further purification.

Figure 1 illustrates the optical absorption spectra of aliquots of the CdSe QDs dissolved in toluene obtained for different times after injected TOP-Se solution into Cd precursor solution. The redshift of the absorption peak of the samples obtained at different time evidence the quantum size effect. The inset of Fig. 1 shows picture of two samples with different QDs size, in a cuvet, illuminated with 475 nm laser. Here, ones can observe the Tyndall effect in colloidal CdSe QDs. The QD size was obtained by using the optical absorption peak, related to first excitonic absorption, and the relation proposed by Willian et al. [44]. Thus, the QDs diameters of set-1, were: 2.16 nm (QD1); 2.26 nm (QD2); 2.31 nm (QD3); 2.40 nm (QD4) and 2.46 nm (QD5).

The ligand exchange reaction method is a common procedure used to functionalize QDs structures [6, 45]. In such a procedure, the native ligands, TOP in our



**Fig. 1** It shows the optical absorption of set-1, CdSe QDs surface stabilized with TOP molecules. The quantum size effect leads to a red-shift of the optical absorption. Inset shows the Tyndall effect in colloidal CdSe QDs.
A 405 nm laser pass thought two solution of toluene contained CdSe QDs of different size
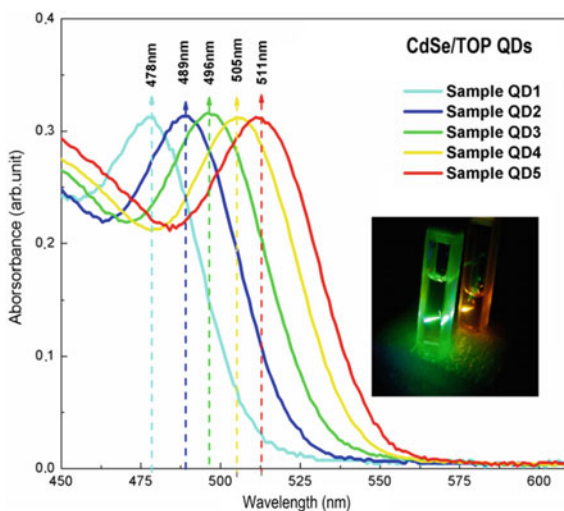
case, are exchanged with less sterically demanding ligands that ideally still impart solution dispersibility and passivate the QDs surface [6, 45].

# 3 Results and Discussion

## 3.1 *Steady-State and Time-Resolved Photoluminescence*

Figure 2a shows the normalized PL spectra, at ordinary room temperature, of CdSe as-synthesized QDs (Set-1) with different sizes. The spectra show the excitonic transition, peaks of high intensity with the spectral position shifted from 490 to 551 nm as a function of QD size, and a broad PL peak at a higher wavelength, around 650 nm. Figure 2b shows the PL spectra of QDs in a lower scale. Here, it is observed that the broad PL peak originates from four transitions, identified as $E_1$, $E_2$, $E_1^s$, and $E_2^s$. The emission at 708 and 768 nm is attributed to well-known deep defect levels, labeled as ($E_1$) and ($E_2$), respectively, for CdSe QDs. Deep defect levels in CdSe QDs with a hexagonal wurtzite structure, a common phase for these materials [46], are related to two energetically different *divacancy* defects, $V_{Cd}$ and $V_{Se}$, associated with the absence of $Cd^{2+}$ and $Se^{2-}$ ions in the crystalline QD structure [47]. One *divacancy* is oriented along the hexagonal *c*-axis of the wurtzite CdSe structure and assigned to trap $E_1$, whereas the other is oriented along the basal
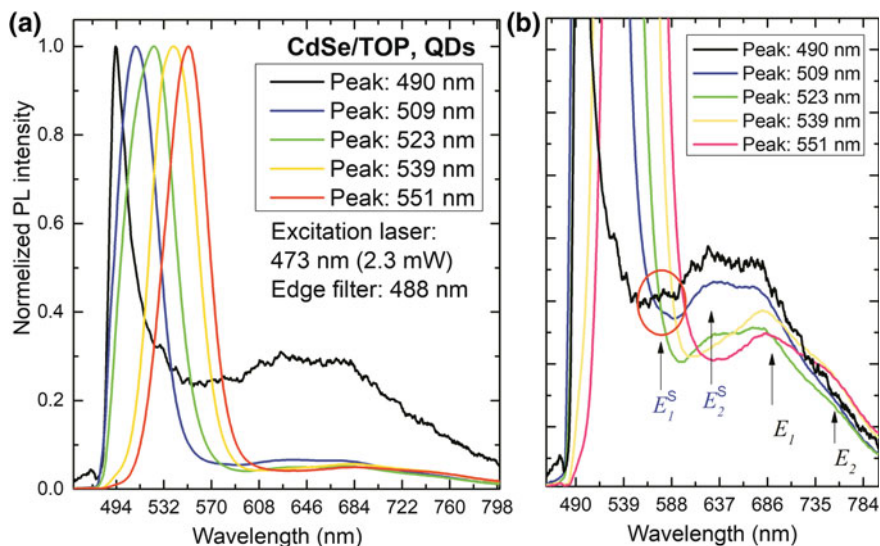


**Fig. 2** (Color online) **a** Normalized PL spectra of CdSe/TOP QDs (set-1—as-synthesized CdSe QDs) with different size obtained at room temperature. **b** Shows a lower scale PL spectra where can be seen four PL peak: vacancy states labelled as $E_1$ and $E_2$, and surface states labelled as $E_1^s$ and $E_2^s$

Cd–Se bond directions and assigned to trap $E_2$ [47]. In addition to the *divacancy* defect, if CdSe QDs are not properly surface passivated, surface trap states could originate from surface defects [28, 48]. Moreover, traps states can originate from an incomplete surface passivation, oxidation of the surface by exposure to air, or by reaction with reducing/oxidizing ligands present in the synthesis reaction [28, 48].

Surface defects have been known for decades to play an important role in QDs, mainly in the energy transfer between the NCs and their environment [29, 49]. For example, in SiO$_2$ NCs, two stable broad luminescence peaks in the visible electromagnetic spectra of the silica NCs have been reported in the past years [50–53] The stable light emission band at approximately 1.79 eV (692 nm) in the silica NCs was assigned to the non-bridging oxygen hole center –NBOHC–($\equiv$Si–O$^*$) at the surface of NCs [50, 52]. The –OH groups on the SiO$_2$ NCs surface are other green emission fonts in SiO$_2$ NCs [51, 53]. The surface states are likely to trap electrons and/or holes, thus inducing recombinations. Therefore, we believe that emissions at 595 nm ($E_1^s$) and at 635 nm ($E_2^s$), shown in Fig. 2b, originated from a localized state due to surface defects in CdSe QDs, one shallow state (S$_1$) and the other deep state (S$_2$) present near the QD conduction and valence bands (VBs), respectively. As the size of the QD decreases, $E_1$ and $E_2$ transitions become less intense than $E_1^s$ and $E_2^s$ transitions, resulting in the broad PL peaks, around 650 nm, to present a blueshift.

Figure 3a shows PL spectra of the CdSe, with different QD sizes, after exchange reaction with HDA ligand. CdSe surface cover with HDA creates new QD surface states [45, 54]. The PL signal of the surface states, relative to excitonic transition, shows higher intensity after surface functionalization and results in a blueshift of the broad PL peak, as shown in Fig. 2a. As the size of the QD decreases, it becomes possible to detect the surface state clearly. Thus, we can tune the localized state from conduction band (for large QD size) to semiconductor band-gap energy (for smaller QD size). In this simple model, the energy of the surface state is static. For QD with larger size and emission at 610 nm, the surface states are into the conduction band (CB) and luminescence is only from excitonic transitions. As the QD size is reduced, the surface states are tuned to the band-gap and their luminescence is more intense, as shown in Fig. 3a. It is important to note that the broad PL peak from surface states is of the same spectral wavelength before and after the surface exchange reaction. Similar results were observed recently in CdTe QDs functionalized with MPA ligand [55]. However, the PL intensity of the surface states improved with relation to the PL intensity of the core-only QDs (surface capped with TOP). This could be interpreted as additional surface states (midgap states) from HDA ligands that improve surface states recombination.

Figure 3b presents normalized PL spectra of CS-QDs as a function of thioglycerol concentration at 16 K. In all spectra, five recombinations can be observed, namely $E_1$, $E_2$, $E_1^s$, $E_2^s$, and the excitonic transition at 487 nm. Here, the excitonic transition has a strong PL quenching effect relative to the PL signal of surface states. In comparison with other two previously discussed QDs sets, new surface ($E_1^s$, and $E_2^s$) and vacancy ($E_1$ and $E_2$) recombinations occur at the sample wavelength as CdSe/TOP QDs (Fig. 2) and CdSe/HDA QDs (Fig. 3a), respectively.
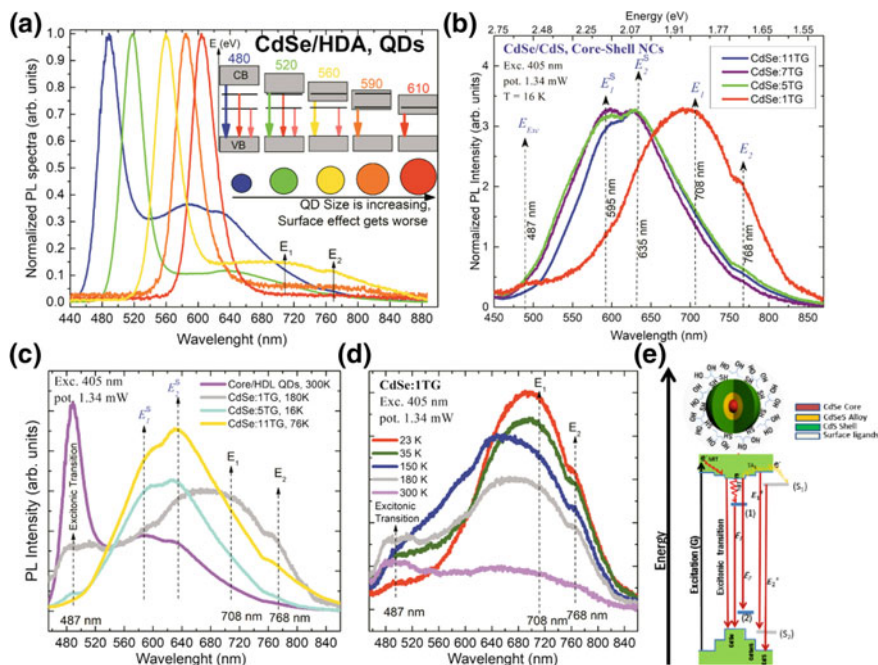
**Fig. 3** Normalized PL spectra of the HDA functionalized CdSe QDs (**a**), at room temperature, and TG-capped CdSe/CdS QDs at 16 K with increasing thioglycerol concentrations (**b**). Their recombination aspects are depicted, where the emissions from both the QD ($E_{exc}$) and the vacancy states ($E_1$) and ($E_2$) are clearly identified. It also shows the characteristic emission from surface states at 595 and 635 nm, $E_1^s$ and $E_2^s$, respectively. **a** Shows electronic surface states tuned from CB to band gap of QDs as QDs size reduction (QDs in quantum confinement regime). **c** Shows, for comparison, the PL spectra of the CdSe HDA functionalized and CS-CdSe with different TG concentration and **d** shows PL spectra of the CdSe:1TG for different temperatures. **e** Depicts the radiative and non-radiative process in the Core-Shell QDs capped with TG. The red arrows represent the non-radiative transitions (NRT) and green arrows represent the thermal activation (TA) processes involving surface states

The sample with 1 TG concentration presents strong vacancy PL intensity (Fig. 3b). As the TG concentration increases, the PL intensity of the surface states increases. Thus, CdSe/CdS structures with 1 TG concentration could have more selenium vacancies than CdSe/CdSe, with a higher TG concentration. CdSe:1TG displays residual dangle-bonds at the QD surface owing to partially capped surface, where virtual QD surface levels (shallow carrier traps) can emit radiations. With the increase in the TG concentration, the PL spectrum of the TG-capped CdSe QDs exhibited significant changes, as subsequent layers of CdS and TG were added to the QD surface. Figure 3c proposes the comparison method of the PL spectra of CdSe/HDA, in magenta, and CS-QDs with different TG concentrations. This figure shows that the surface and vacancy transitions are in the same energy position as CS-QDs or CdSe/HDA. Figure 3d presents the PL spectra of CdSe:1TG at different

temperatures. Here, one can observe the energy transfer from deeper localized states to surface states, depicting energy proximity between the states.

It is known that thiols form an important class of capping molecules; they have a polar head group and are used to synthesize water-soluble QDs. However, thiols can also introduce surface electronic levels (trap states) on the QD surface [5]. For instance, a recent work demonstrated that the hybridization intensity of the surface states in the QD systems could control energy position of VB and CB [28, 54]. Previous studies on CdSe QDs capped with the thiol group have particularly observed two radiative emission peaks near 600 and 640 nm, which are characteristic of CdSe QDs smaller than 3.6 nm [32, 55]. Also, emissions with a peak at around 595 nm (labeled in this article by $E_1^s$) and at 635 nm (by $E_2^s$), as shown in Figs. 2b, 3a, b, originated from localized surface states from different groups with similar energies. Thus, an increase in the concentration of thiols may, in principle, lead to an increase in the localized surface states, and subsequently an improvement in the surface PL signal, as shown in Fig. 3b.

When TG concentration was increased from 1 to 5 mmol, the surface shielding, in particular, improved, i.e., incomplete bonds and defect states levels reduced [56, 57]. At this moment, a *thin* shell of CdSe$_x$S$_{1-x}$ developed around the CdSe core. Hence, the stabilizer, thioglycerol molecules, localized the electronic levels in the CdS surface that could be coupled by charge tunneling, depending on the shell thickness. The charge tunneling was then changed from the CdS surface to the CdSe core. This quantum process could increase the probability of non-radiative electron–hole recombination up to a specific shell thickness, a finding consistent with other studies [5, 58].

A study reported that the creation of electron trap states on the QD surface following the binding of the thiol functional group significantly influenced the electron transfer kinetics [59]. Recent analyses of QD–ligand interactions have reported delocalization of the charge-carrier wave functions onto organic ligands based on the ligand structure and functional group, specifically stressing on the hole-accepting ability of amine functional groups [54, 60]. Thus, the passivation of QDs with thioglycerol has been shown to create electron-trapping states on the QD [5, 29]. Different studies have shown that thiol ligands bind very strongly to the cadmium atoms on the surface of CdSe QDs [6]. Moreover, it has been demonstrated that thiol and thiolate ligands act as photogenerated hole traps and passivate electron traps [61]. Wuister et al. [62], and Baker et al. [29], have shown that hole trapping is the principal process for excitonic PL quenching in CdSe QDs capped with thiols. On the contrary, recent studies reported that graded alloy CdSe/CdSe$_x$S$_{1-x}$/CdS structure, with a *thick*-shell, could suppress hole-trapping process, reducing the non-radiative Auger recombination and subsequently improving the excitonic pholuminescence efficiency [30, 38].

In our synthesis process, the CdSe/CdSe$_x$S$_{1-x}$/CdS shell was constructed using 1-thioglycerol. In this process, the existence of residual thiol ligands on the CdSe/CdSe$_x$S$_{1-x}$/CdS surface resulted in a higher hole-trapped states density. As the shell was thin, we believe that charge tunneling from QD to surface states could have

occurred. This cannot occur in a thick-shell structure. The CdSeS/CdS shell structure form a quasi-type-II band structure of the graded alloy CdSSe QDs in which the excess electron energy (photoexcited in the PL experiment) in the CB is greater than the confinement potential of the CB offset of only $\sim 0.0$–0.1 eV between the CdSe core and the CdS shell [38]. Therefore, the electron is delocalized throughout both the core and shell materials. Figure 3e shows an illustrative band alignment and the radiative and non-radiative processes in the core-shell QDs capped with TG. The red arrows represent the non-radiative transitions (NRTs) and green arrows represent the thermal activation (TA) processes involving surface states.

In an analysis of electron transfer kinetics at the QD–metal oxide interface in CdSe QDs capped with MPA, Hines and Kamat [5, 63], showed that MPA created electron-trapping states on the surface of CdSe QDs. This is evident from the formation of shallow $S_1$ states, as shown in Fig. 3e. Recently, Frederick et al. [54, 64], proposed, within second-order perturbation theory and experimental data, a strong electronic coupling between delocalized orbitals of the VB of CdSe QDs and the HOMO orbitals of capping ligands. The mixing of ligand orbitals with the orbitals of the QD that are delocalized over both core and surface generates new hybridized orbitals that split the states from energies of isolated orbitals [38]. These results show that surface states in QDs can couple with electronic states of QDs, leading to new possibilities for charge transfer from the surface to the nucleus or vice versa. Moreover, the new hybridized states can be tunneled to QD outside the band gap, leading to QD surface functionalization [28].

Figure 4 shows the fluorescence decay of CdSe:xTG (x = 1, 5, 7, 9 and 11 mmol) with decays monitored at 635 nm and emission of $E_2^s$, (Fig. 4a). The PL decay from the CdSe capped QDs had a multi-exponential form, a finding consistent with earlier studies [5, 25, 65, 66]. The lifetime traces were fitted to a tri-exponential decay function, resulting in long ($\tau_1 \sim 23.0$ ns), medium ($\tau_2 \sim 3.5$ ns), and short ($\tau_3 \sim 0.36$ ns) lifetimes using the following equation: ($I = A_1 \exp(-t/\tau_1) + A_2 \exp(-t/\tau_2) + A_3 \exp(-t/\tau_3)$), where $I$ is the emission intensity; $A_1$, $A_2$, and $A_3$ are pre-exponential factors; and $\tau_1$, $\tau_2$, and $\tau_3$ are the lifetimes. The lifetime of channel 1 was similar to that of the core-only CdSe QDs (22.0 ns; obtained from samples presented in Fig. 2a).

Channel 3 with a lifetime of $\sim 0.36$ ns ($\tau_3$) is similar to that reported for biexciton recombination in CdSe/CdSe/CdSe$_x$CdS$_{1-x}$/CdS [65, 67]. In the biexciton recombination, a non-radiative process, the Auger decay and the lifetime increased with QD volume [67]. For CdSe/CdS CS QD, the biexciton lifetime ($\tau_{2x}$) increased from 60 ps to 23 ns with an increase in the shell thickness from 0.0 to 5.6 nm [67]. Similar results were observed in the present study, as shown in Fig. 4a. However, the shell of our samples was lower. Figure 4a shows that as the thickness of the shell increases, the suppression of the Auger recombination increases, similar to that observed early [68]. This is an evidence of alloy formation between CdSe and the CdS shell.
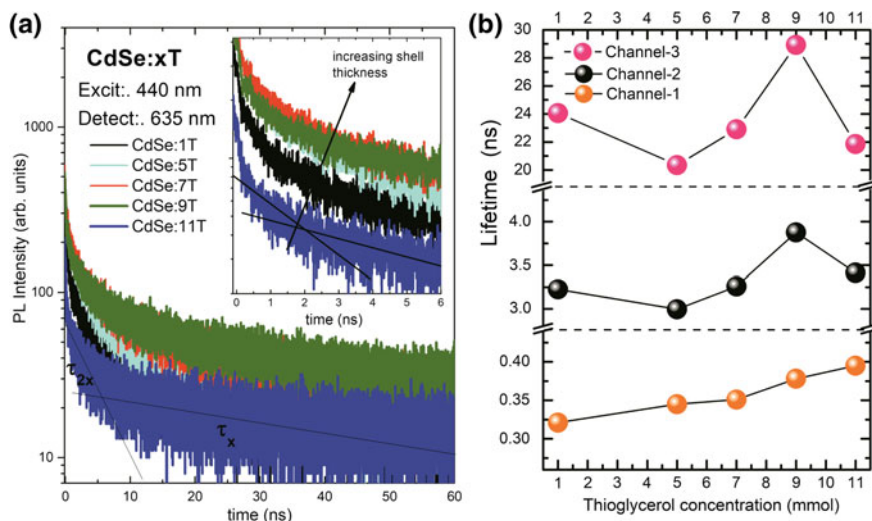
**Fig. 4** **a** The fluorescence decay curves as a function of thioglycerol concentration for detection at 635 nm. The lifetime was obtained after a fitting procedure with a triexponential decay. **b** Life time for tree different channels as a function of thioglycerol concentration

Figure 4a, b shows that the average lifetime increased from 1 to 7 mmol of thioglycerol concentration and decreased at higher concentrations (see general behavior of fluorescence decay curves). Recent measurements of steady-state fluorescence in CdSe CS-QDs, with increasing concentration of thioglycerol, have shown that the fluorescence intensity increased as the thioglycerol concentration increased from 1 to 9 mmol, and it decreased at 11 mmol concentration [42], similar to the results observed in our lifetime data.

It is known that localized states proximal to or resonant with the extended states of CB have similar lifetimes. In this case, the lowest energy state, a localized state with longer lifetime, can serve as a charge reservoir for the state with a shorter lifetime. This charge reservoir could be accessed by thermal activation [69]. Lifetimes similar to that obtained in our experimental data were recently obtained by Mohamed et al., when analyzing the recombination of thiol-capped CdS nanoparticle films [70].

## 3.2 Photoluminescence as a Function of Temperature: Thermal Carrier Transfer

To further study the emissions at 595 and 635 nm from the surface states of TG-capped CdSe QDs, we analyzed PL as a function of temperature. Figures 5a, b shows the energy transfer process among surfaces states and the CS-QDs band edge
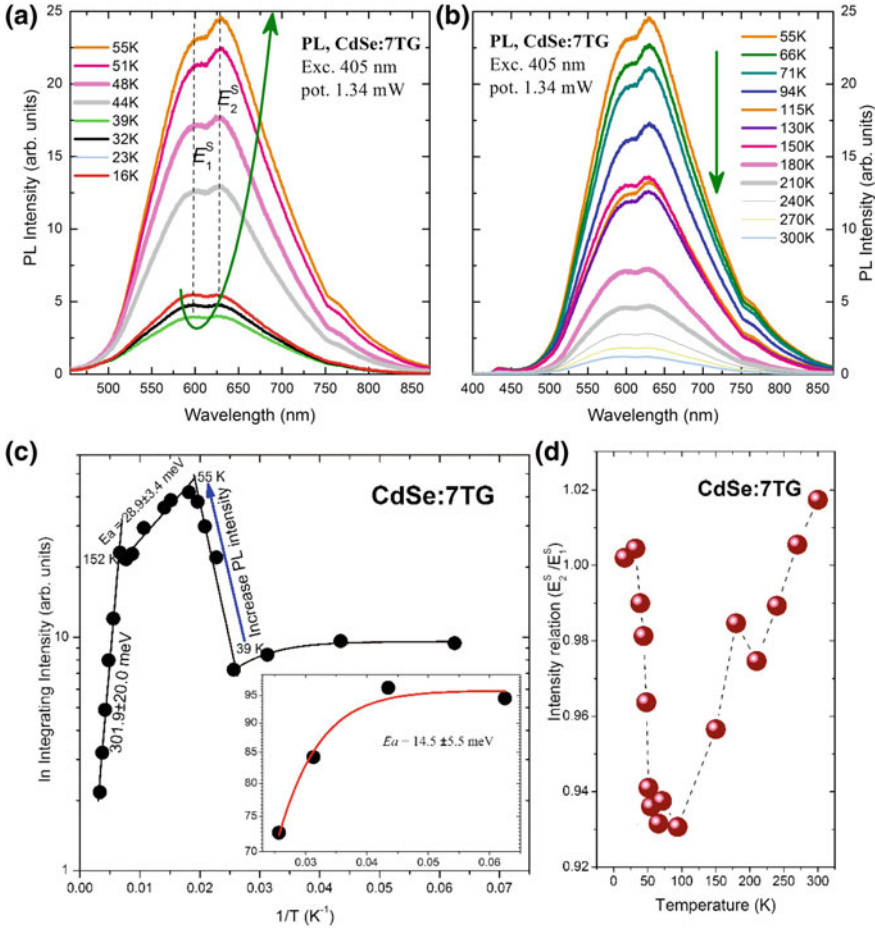
**Fig. 5** **a**, **b** Show PL spectra of CdSe:7TG as a function of temperature. **c** shows integrated PL intensity as a function of 1/T for CdSe:7TG. The inset shows an expanded linear scale in the low temperature interval. The red line, in the inset, represents the best fit of a phenomenological expression: $I(T) = I_0 / \left[1 + A \exp\left(-\frac{Ea}{KT}\right)\right]$ [71, 72], Here *Ea* is the thermal activation energy and K is the Boltzmann constant. **d** Shows the relation of the PL peak intensity between $E_2^s$ and $E_1^s$ as a function of temperature

state. From 16 to 39 K, the PL spectrum depicts a reasonable intensity reduction as the temperature increases, a natural behavior for semiconductor materials. From 39 to 55 K, the PL intensity undergoes a sudden and unexpected increase, which, however, is not symmetrical between the components $E_1^s$ and $E_2^s$. In this case, the increase in the emission intensity of $E_2^s$ is more than that in the emission intensity of $E_1^s$. This behavior can be seen in Fig. 5d. For temperatures higher than 55 K, the intensity of the PL decreases. These PL(T) behaviors show the complex processes

of energy transfer by thermal activation of electronic states in CdSe:xTG materials and involve delocalized states of QDs and localized states of the capping agent.

Figure 5c shows the integrated PL intensity of CdSe:7TG sample as a function of inverse temperature. From 16 to 39 K, the PL intensity undergoes a moderate thermal quenching with an activation energy of 14.5 meV. We believe thermal quenching is relatively weaker in this temperature interval owing to the transfer of charge carriers from $S_1$ states to the electronic levels of QD via thermal activation TA$_1$, as shown in Fig. 3e. This low activation energy reflects proximity between the $S_1$ states and the electronic level of CS-QDs. However, at 39 K, the integrated PL intensity rapidly increases until 55 K, where it attains the thermal activation of a non-radiative channel have an energy barrier of about 28.9 meV (between 55 and 152 K). Hence, we found that the thermal activation energy of 39 K at TA$_2$ is sufficient to overcome the potential barrier between the electronic states of the CdSe core and the CdS shell. As shown in Fig. 5b, activation energy of approximately 28.9 meV in this simple model provides the thermal energy to pump holes of the $S_2$ state on the top of the VB, thereby significantly reducing the emission intensity $E_2^s$ than the emission $E_1^s$, in agreement with the PL peak evolution for different temperatures. Figure 2c depicts the thermal activation energy TA$_3$. From 152 K, integrated PL intensity undergoes another thermal quenching process, causing the intensity to rapidly decrease with temperature. This process has activation energy of 301.9 meV and may be associated with non-radiative vacancy states.

## 4   Conclusions

Three sets of CdSe quantum dots (QDs) covered with different ligand molecules were growth and analyzed by optical spectroscopy. Set-1 (as-synthesized QDs) is composed by five samples of CdSe with size between 2.16 nm and 2.46 nm covered by TOP. Set-2 is composed by five samples of CdSe QDs, Set-1, functionalized, after exchange reaction process, with HDA molecules. Set-3 is composed by CdSe/CdSe$_x$S$_{1-x}$/CdS alloyed, core-shell (CS-QDs) capped with different thioglycerol concentration, a different synthesis process. All these sets present luminescence of ligand states (surfaces, and vacancy $E_1$, $E_2$ states) and excitonic transitions. Interestingly, all surfaces ($E_1^s$ and $E_2^s$) and vacancy ($E_1$, $E_2$) recombinations occur at sample energy position for the three set of QDs. Similar results were observed recently in CdTe QDs functionalized with MPA ligand [55]. However, the PL intensity of the surface states, in CS-QDs, are interestingly improved with relation to PL intensity of the core-only QDs (surface capped with TOP).

Anomalous increases in the luminescence intensity of the core-shell QDs, with increasing temperature, and a continuous redshift in the optical absorption peak, as a function of ligand concentration, evidence a strong electronic coupling between surface localized orbitals and delocalized excitonic CdSe QD states. Thus, we

believe that both shell of CdS as thiol states on the surface of CS-QDs can serves as a reservoir of charges to the core of CdSe. We believe that the main results of our paper will be useful to many groups working in this field, stimulating further investigations and applications mainly in the control of the carrier pathways after its photo- or electric-excitation in core-shell quantum dots that can be an important strategy to improve efficiency of photovoltaic or photodetector devices.

# References

1. Talapin, D.V., Haubold, S., Rogach, A.L., Kornowski, A., Haase, M., Weller, H.: J. Phys. Chem. B **105**, 2260–2263 (2001)
2. Talapin, D.V., Rogach, A.L., Kornowski, A., Haase, M., Weller, H.: Highly luminescent monodisperse CdSe and CdSe/ZnS nanocrystals synthesized in a hexadecylamine- tri-octylphos- phine oxide- trioctylphospine mixture. Nano lett. **1**, 207–211 (2001)
3. Murray, C.B., Norris, D.J., Bawendi, M.G.: Synthesis and characterization of nearly monodis–perse CdE (E = sulfur, selenium, tellurium) semiconductor nanocrystallites. J. Am. Chem. Soc. **115**, 8706–8715 (1993)
4. Alivisatos, A.P.: Semiconductor clusters, nanocrystals, and quantum dots. Science **271**, 933–937 (1996)
5. Hines, D.A., Kamat, P.V.: Quantum dot surface chemistry: ligand effects and electron transfer reactions. J. Phys. Chem. C **117**, 14418–14426 (2013)
6. Buckley, J.J., Couderc, E., Greaney, M.J., Munteanu, J., Riche, C.T., Bradforth, S.E., Brutchey, R.L.: Chalcogenol ligand toolbox for CdSe nanocrystals and their influence on exciton relaxation pathways. ACS Nano **8**, 2512–2521 (2014)
7. Colvin, V.L., Schlamp, M.C., Alivisatos, A.P.: Light-emitting diodes made from cadmium se-lenide nanocrystals and a semiconducting polymer. Nature **370**, 354–357 (1994)
8. Park, S.S., Kim, D.H., Jeon, Y.P., Kim, T.W.: Enhancement of the stabilization in white organic light-emitting diodes utilizing a color conversion layer containing CdSe/ZnS quantum dots. J. Nanosci. Nanotechnol. **13**, 7194–7197 (2013)
9. Kim, Y., Greco, T., Ippen, C., Wedel, A., Oh, M.S., Han, C.J., Kim, J.: Indium phosphide-based colloidal quantum dot light-emitting diodes on flexible substrate. Nanosci. Nanotechnol. Lett. **5**, 1065–1069 (2013)
10. Shen, H.B., Lin, Q.L., Wang, H.Z., Qian, L., Yang, Y.X., Titov, A., Hyvonen, J., Zheng, Y., Li, L.S.: Efficient and bright colloidal quantum dot light-emitting diodes via controlling the shell thickness of quantum dots. ACS Appl. Mater. Interfaces **5**, 12011–12016 (2013)
11. Klimov, V.I., Mikhailovsky, A.A., Xu, S., Malko, A., Hollingsworth, J.A., Leatherdale, C.A., Eisler, H.J., Bawendi, M.G.: Optical gain and stimulated emission in nanocrystal quantum dots. Science **290**, 314–317 (2000)
12. Harrison, M.T., Kershaw, S.V., Burt, M.G., Rogach, A.L., Kornowski, A., Eychmuller, A., Weller, H.: Colloidal nanocrystals for telecommunications. complete coverage of the low-loss fiber windows by mercury telluride quantum dot. Pure Appl. Chem. **72**, 295–307 (2000)
13. Thon, S.M., Sargent, E.H.: In: Eldada, L.A. (ed.) Thin Film Solar Technology, 3rd edn. (2011)
14. Tang, J.A., Sargent, E.H.: Infrared colloidal quantum dots for photovoltaics: fundamentals and recent progress. Adv. Mater. **23**, 12–29 (2011)
15. Li, X.M., Li, Y.F., Zeng, H.B.: Multiexciton generation in semiconductor nanocrystals: a potential avenue toward efficient solar cells. Sci. Adv. Mater. **5**, 1585–1595 (2013)
16. Chen, Z., Zhang, H., Yu, W., Li, Z., Hou, J., Wei, H., Yang, B.: Inverted hybrid solar cells from aqueous materials with a PCE of 3.61%. Adv. Energy Mater. **3**, 433–437 (2013)

17. Zhao, L., Hu, L., Fang, X.: Growth and device application of CdSe nanostructures. Adv. Funct. Mater. **22**, 1551–1566 (2012)
18. Bruchez, M., Moronne, M., Gin, P., Weiss, S., Alivisatos, A.P.: Semiconductor nanocrystals as fluorescent biological labels. Science **281**, 2013–2016 (1998)
19. Dong, M.T., Fu, S.S., Liu, S.X., Xu, J.Y., Huang, C.B.: One-pot synthesis of CdSe quantum dots in aqueous solution for biological labeling. J. Chin. Chem. Soc. **60**, 1328–1332 (2013)
20. Almeida Silva, A.C., Barbosa Silva, M.J., Cordero da Luz, F.A., Silva, D.P., Vieira de Deus, S.L., Dantas, N.O.: Controlling the cytotoxicity of CdSe magic-sized quantum dots as a function of surface defect density. Nano Lett. **14**, 5452–5457 (2014)
21. Xiu, Z.-M., Zhang, Q.-B., Puppala, H.L., Colvin, V.L., Alvarez, P.J.: Negligible particle-specific antibacterial activity of silver nanoparticles. Nano Lett. **12**, 4271–4275 (2012)
22. He, S.-J., Cao, J., Li, Y.-S., Yang, J.-C., Zhou, M., Qu, C.-Y., Zhang, Y., Shen, F., Chen, Y., Li, M.-M., Xu, L.-M.: World J. Gastroenterol. **22**, 5012–5022 (2016)
23. Kim, B.H., Hackett, M.J., Park, J., Hyeon, T.: Synthesis, characterization, and application of ultrasmall nanoparticles. Chem. Mater. **26**, 59–71 (2014)
24. Kamat, P.V., Christians, J.A., Radich, J.G.: Quantum dot solar cells: hole transfer as a limiting factor in boosting the photoconversion efficiency. Langmuir **30**, 5716–5725 (2014)
25. Yun, H.J., Paik, T., Edley, M.E., Baxter, J.B., Murray, C.B.: Enhanced charge transfer kinetics of CdSe quantum dot-sensitized solar cell by inorganic ligand exchange treatments. ACS Appl. Mater. Interfaces. **6**, 3721–3728 (2014)
26. Li, X., Feng, D., Tong, H., Jia, T., Deng, L., Sun, Z., Xu, Z.: Hole surface trapping dynamics directly monitored by electron spin manipulation in CdS nanocrystals. J. Phys. Chem. Lett. **5**, 4310–4316 (2014)
27. Maity, P., Debnath, T., Ghosh, H.N.: Slow electron cooling dynamics mediated by electron–hole decoupling in highly luminescent CdS$_x$Se$_{1-x}$ alloy quantum dots. J. Phys. Chem. C **119**, 10785–10792 (2015)
28. Houtepen, A.J., Hens, Z., Owen, J.S., Infante, I.: On the origin of surface traps in colloidal II–VI semiconductor nanocrystals. Chem. Mater. **29**, 752–761 (2017)
29. Baker, D.R., Kamat, P.V.: Tuning the emission of CdSe quantum dots by controlled trap enhancement. Langmuir **26**, 11272–11276 (2010)
30. Park, Y.-S., Bae, W.K., Padilha, L.A., Pietryga, J.M., Klimov, V.I.: Effect of the core/shell interface on auger recombination evaluated by single-quantum-dot spectroscopy. Nano Lett. **14**, 396–402 (2014)
31. Lu, H., Joy, J., Gaspar, R.L., Bradforth, S.E., Brutchey, R.L.: Iodide-passivated colloidal PbS nanocrystals leading to highly efficient polymer: nanocrystal hybrid solar cells. Chem. Mater. **28**, 1897–1906 (2016)
32. Larson, D.R., Zipfel, W.R., Williams, R.M., Clark, S.W., Bruchez, M.P., Wise, F.W., Webb, W.W.: Water-soluble quantum dots for multiphoton fluorescence imaging in vivo. Science **300**, 1434–1436 (2003)
33. Pelley, J.L., Daar, A.S., Saner, M.A.: State of academic knowledge on toxicity and biological fate of quantum dots. Toxicol. Sci. **112**, 276–296 (2009)
34. Kim, S., Fisher, B., Eisler, H.J., Bawendi, M.: Type-II quantum dots: CdTe/CdSe(core/shell) and CdSe/ZnTe(core/shell) heterostructures. J. Am. Chem. Soc. **125**, 11466–11467 (2003)
35. Chen, O., et al.: Compact high-quality CdSe–CdS core–shell nanocrystals with narrow emission linewidths and suppressed blinking. Nat. Matter. **12**, 445–451 (2013)
36. McBride, J., Treadway, J., Feldman, L.C., Pennycook, S.J., Rosenthal, S.J.: Structural basis for near unity quantum yield core/shell nanostructures. Nano Lett. **6**, 1496–1501 (2006)
37. Gong, K., Kelley, D.F.: Lattice strain limit for uniform shell deposition in zincblende CdSe/CdS quantum dots. J. Phys. Chem. Lett. **6**, 1559–1562 (2015)
38. Keene, J.D., McBride, J.R., Orfield, N.J., Rosenthal, S.J.: Elimination of hole–surface overlap in graded CdS$_x$Se$_{1-x}$ nanocrystals revealed by ultrafast fluorescence upconversion spectroscopy. ACS Nano **8**, 10665–10673 (2014)

39. Garcia-Santamaria, F., Chen, Y., Vela, J., Schaller, R.D., Hollingsworth, J.A., Klimov, V.I.: Suppressed auger recombination in "giant" nanocrystals boosts optical gain performance. Nano Lett. **9**, 3482–3488 (2009)
40. Wang, X.Y., Ren, X.F., Kahen, K., Hahn, M.A., Rajeswaran, M., Maccagnano-Zacher, S., Silcox, J., Cragg, G.E., Efros, A.L., Krauss, T.D.: Non-blinking semiconductor nanocrystals. Nature **459**, 686–689 (2009)
41. Lawrence, K.N., Dutta, P., Nagaraju, M., Teunis, M.B., Muhoberac, B.B., Sardar, R.: Dual role of electron-accepting metal-carboxylate ligands: reversible expansion of exciton delocalization and passivation of nonradiative trap-states in molecule-like CdSe nanocrystals. J. Am. Chem. Soc. **138**, 12813–12825 (2016)
42. Silva, A.C.A., da Silva, S.W., Morais, P.C., Dantas, N.O.: Shell thickness modulation in ultrasmall $CdSe/CdS_xSe_{1-x}/CdS$ core/shell quantum dots via 1-Thioglycerol. ACS Nano **8**, 1913–1922 (2014)
43. Donega, C.M., Liljeroth, P., Vanmaekelbergh, P.: Physicochemical evaluation of the hot-injection method, a synthesis route for monodisperse nanocrystals. Small **1**(12), 1152–1162 (2005)
44. W. Willian, Y., et al.: Experimental Determination of the Extinction Coefficient of CdTe, CdSe, and CdS Nanocrystals. vol. 125, pp. 2854–2860 (2003)
45. Boles, M.A., Ling, D., Hyeon, T., Talapin, D.V.: The surface science of nanocrystals. Nature mater. **15**, 141–153 (2016)
46. Babentsov, V., Riegler, J., Schneider, J., Ehlert, O., Nann, T., Fiederle, M.: Deep level defect luminescence in cadmium selenide nano-crystals films. J. Cryst. Growth **280**, 502–508 (2005)
47. Freitas Neto, E.S., Dantas, N.O., Barbosa Neto, N.M., Guedes, I., Chen, F.: Control of luminescence emitted by $Cd_{1-x}Mn_xS$ nanocrystals in a glass matrix: x concentration and thermal annealing. Nanotechnology **22** (2011)
48. Henglein, A.: Physicochemical properties of small metal particles in solution: "microelectrode" reactions, chemisorption, composite metal particles, and the atom-to-metal transition. J. Phys. Chem. **97**, 5457–5471 (1993)
49. Rosa, I.L.V., Nassar, E.J., Serra, O.A.: $Eu^{3+}$ and $Tb^{3+}$ organophosphonates: synthesis, characterization and luminescent properties. J. Alloy. Compd. **275**, 315–317 (1998)
50. Glinka, Y.D., Lin, S.H., Chen, Y.T.: Time-resolved photoluminescence study of silica nanoparticles as compared to bulk type-III fused silica. Phys. Rev. B **66**, 035404 (2002)
51. Zhao, Q.C., Chen, W.M., Zhu, Q.R.: Self-assembly and characterization of novel amorphous $SiO_x$ (x = 2.1) nanospheres. Nanotechnology **15**, 958–961 (2004)
52. Rahman, I.A., Vejayakumaran, P., Sipaut, C.S., Ismail, J., Chee, C.K.: Size-dependent physico-chemical and optical properties of silica nanoparticles. Mater. Chem. Phys. **114**, 328–332 (2009)
53. Lourenco, S.A., Laureto, E., Andrade, A.A., Silva, A.C.A., Dantas, N.O.: Efficient energy transfer mediated by intrinsic SiO2 nanocrystals in $Eu^{+3}$-doped lead borosilicate glasses. Mater. Chem. Phys. **139**, 471–477 (2013)
54. Frederick, M.T., Amin, V.A., Swenson, N.K., Ho, A.Y., Weiss, E.A.: Control of exciton confinement in quantum dot–organic complexes through energetic alignment of interfacial orbitals. Nano Lett. **13**, 287–292 (2013)
55. Vale, B.R.C., Silva, F.O., Carvalho, M.S., Raphael, E., Ferrari, J.L., Schiavon, M.A.: Water-soluble cdte/cds core/shell semiconductor nanocrystals: how their optical properties depend on the synthesis methods. Crystals **6**, 133 (2016)
56. Pal, M., Mathews, N.R., Santiago, P., Mathew, X.: A facile one-pot synthesis of highly luminescent CdS nanoparticles using thioglycerol as capping agent. J. Nanopart. Res. **14**, 916 (2012)
57. Wuister, S.F., Meijerink, A.: Synthesis and luminescence of CdS quantum dots capped with a silica precursor. J. Lumin. **105**, 35–43 (2003)
58. Liu, I.-S., Lo, H.-H., Chien, C.-T., Lin, Y.-Y., Chen, C.-W., Chen, Y.-F., Su, W.-F., Liou, S.-C.: Enhancing photoluminescence quenching and photoelectric properties of CdSe quantum dots with hole accepting ligands. J. Mater. Chem. **18**, 675–682 (2008)

59. Turk, M.E., et al.: Ultrafast electron trapping in ligand-exchanged quantum dot assemblies. ACS Nano **9**, 1440–1447 (2015)
60. Tan, Y., Jin, S., Hamers, R.J.: Influence of hole-sequestering ligands on the photostability of CdSe quantum dots. J. Phys. Chem. C **117**, 313–320 (2012)
61. Knowles, K.E., Tice, D.B., McArthur, E.A., Salomon, G.C., Weiss, E.A.: Chemical control of the photoluminescence of CdSe quantum dot-organic complexes with a series of para-substituted aniline ligands. J. Am. Chem. Soc. **132**, 1041–1050 (2019)
62. Wuister, S.F., Donega, C., Meijerink, A.: Influence of thiol capping on the exciton luminescence and decay kinetics of CdTe and CdSe quantum dots. J. Phys. Chem. B **108**, 17393–17397 (2004)
63. Frederick, M.T., Amin, V.A., Cass, L.C., Weiss, E.A.: A molecule to detect and perturb the confinement of charge carriers in quantum dots. Nano Lett. **11**, 5455–5460 (2011)
64. Hines, D.A., Kamat, P.V.: Recent advances in quantum dot surface chemistry. ACS Appl. Mater. Interfaces **6**, 3041–3057 (2014)
65. Dibbell, R.S., Watson, D.F.: Distance-dependent electron transfer in tethered assemblies of CdS quantum dots and TiO$_2$ nanoparticles. J. Phys. Chem. C **113**, 3139–3149 (2009)
66. Robel, I., Subramanian, V., Kuno, M., Kamat, P.V.: Quantum dot solar cells. harvesting light energy with CdSe nanocrystals molecularly linked to mesoscopic TiO$_2$ films. J. Am. Chem. Soc. **128**, 2385–2393 (2006)
67. Bae, W.K., et al.: Controlled alloying of the core–shell interface in CdSe/CdS quantum dots for suppression of auger recombination. ACS Nano **7**, 3411–3419 (2013)
68. García-Santamaría, F., Brovelli, S., Viswanatha, R., Hollingsworth, J.A., Htoon, H., Crooker, S.A., Klimov, V.I.: Breakdown of volume scaling in auger recombination in CdSe/CdS heteronanocrystals: the role of the core- shell interface. Nano Lett. **11**, 687–693 (2011)
69. Vlaskin, V.A., Janssen, N., van Rijssel, J., Beaulac, R., Gamelin, D.R.: Tunable dual emission in doped semiconductor nanocrystals. Nano Lett. **10**, 3670–3674 (2010)
70. Mohamed, N.B.H., Haouari, M., Zaaboub, Z., Nafoutti, M., Hassen, F., Maaref, H., Ben Ouada, H.: Time resolved and temperature dependence of the radiative properties of thiol-capped CdS nanoparticles films. J. Nanoparticle Res. **16**, 2242 (2014)
71. Leroux, M., Grandjean, N., Beaumont, B., Nataf, G., Semond, F., Massies, J., Gibart, P.: Temperature quenching of photoluminescence intensities in undoped and doped GaN. J. Appl. Phys. **86**, 3721–3728 (1999)
72. Lourenco, S.A., Dias, I.F.L., Pocas, L.C., Duarte, J.L., de Oliveira, J.B.B., Harmand, J.C.: Effect of temperature on the optical properties of GaAsSbN/GaAs single quantum wells grown by molecular-beam epitaxy. J. Appl. Phys. **93**, 4475–4479 (2003)